A Novel Compact Polarization Diversity Ultra-Wideband MIMO Antenna

Saeid Karamzadeh [1,2]

[1] Application & Research Center for Advanced Studies, Istanbul Aydin University, Turkey
[2] Department of Electrical and Electronics Engineering, Istanbul Aydin University, Turkey

Abstract ─ A very compact modified simple structure Ultra-Wideband (UWB) antenna with a size of 18 mm by 30 mm is presented for polarization diversity applications. The antenna employs two orthogonal monopole antenna to achieve polarization diversity over the UWB. The antenna was fabricated to study the performance such as S-parameters, radiation pattern, radiation efficiency, peak gain, envelope correlation coefficient and group delay. The measured results demonstrated that the proposed antenna has not only UWB (147.96% impedance bandwidth) but also good isolation less than about -25 dB. Moreover, the system fidelity factor is sufficient for pulse transmission with average 89.6% and 85.3% for ports 1 and 2, respectively. Furthermore, a low envelope correlation coefficient of less than 0.001 occurred, too. All these features show that the proposed UWB MIMO antenna can meet the requirement of MIMO/diversity of communication applications well.

Index Terms ─ Microstrip feed, monopole antenna, polarization diversity, UWB.

I. INTRODUCTION

The rapid developments in modern wireless communication systems demand a high data rate, strong dependability and heftiness. Ultra-wideband (UWB) technique is one of the most important technologies in indoor communications in order to have benefits such as low susceptibility to multipath fading, reduced probability of detection and intercept, and potentially high data rates [1-7]. But similar to most of the wireless communication systems, UWB systems usually suffer from channel fading caused by multipath environment [1-7]. To solve this problem, Multiple-Input-Multiple-Output (MIMO) technology is developed to supply best coverage and to become better performance over multipath wireless channels by utilizing multiple antennas at the transmitter and receiver [5-9]. The main problem facing the implementation of MIMO technology is the limited space available at each end of the communication link. Saving this extra space may cause performance degradation; therefore, polarization diversity needs to be considered in true wireless channels. These advantages enable UWB antenna to change polarization diversity by its capability attractive for wireless body area networks (WBANs). An appropriate UWB-WBAN diversity antenna must have low mutual coupling, i.e., high isolation between its branches [10]. The higher isolation leads to better diversity performance and higher efficiency of each branch. Hitherto, various techniques to attain UWB diversity antennas have been investigated and reported, aimed at reducing the antenna size and increasing the isolation [1-7]. In [1], a uniplanar, UWB dual-polarized antenna embedded with narrowband reject filter is presented. A style of designing ground plane has resulted in an enhance antenna foot print to 58×58×1.524 mm^3. Isolation between two ports is less than -15 dB. In [3, 4], by using a similar radiation patch, two type of UWB polarization diversity antenna in different large size and number in elements are provided (details is given in Table 1). In [5], a large size (50×50×1.524 mm^3) CPW fed uniplanar antenna with frequency range from 2.76 to 10.75 GHz and a rejection performance in the frequency band 4.75–6.12 GHz, along with isolation better than 15 dB, is reported. In [11] and [12], two UWB tapered slot antennas (TSAs) and mutual coupling below 15 dB are developed. That design utilizes a spatial diversity technique and, to the authors' knowledge, has the smallest size (27×47 mm^2) among the recently designed UWB diversity antennas. It should be noted that although a printed cantor set fractal antenna using spatial diversity, proposed in [13], has a smaller size (25×48 mm^2), its bandwidth is 80% of the UWB frequency defined range. In [7], a smaller UWB polarization antenna than reported works until the time of its release was worked. That is 52×27 mm^2 in size, and isolation between two input ports is less than -22 dB. In this work, we present a low profile 18×30×1.6 mm^3, small size polarization diversity antenna with covering impedance bandwidth from 2.97 to 19.86 GHz. This antenna with isolation less than about -25 dB between two ports and correlation coefficient less than -30 dB is a good choice for wireless systems which needs polarization diversity application. The proposed antenna has an area of 540 mm^2, which is significantly less than the recently published UWB polarization diversity antenna, as summarized in Table 1. Compared to other

Submitted On: October 9, 2016
Accepted On: December 6, 2016

similar types of antennas, the proposed antenna displays an impedance bandwidth which is significantly larger and shows no reduction in the gain performance as well as having better other results.

Table 1: Comparison of the proposed antenna with same works (IBW is Impedance Bandwidth, Sij is Isolation, ECC is Envelope Correlation Coefficient, FF is Fidelity Factor, GD is Group Delay, PW is Proposed Work, and RE is Radiation Efficiency)

Ref.	Size (mm)	IBW (GHz)	S_{ij} (dB)	ECC	FF (%)	Gain (dBi)	GD (ns)	RE (%)
[1]	58×58	8.2 GHz	-14	0.025	80	2.2	1	85
[3]	48×48	8.7 GHz	-15	0.04	--	~3	--	80
[4]	65×65	8.25 GHz	-40	--	--	~6.5	--	--
[5]	50×50	7.99 GHz	-15	0.025	95	~5.5	1	75
[6]	64×64	8 GHz	-40	0.006	--	~6.5	1	75
[7]	27×52	8.75 GHz	-22	0.01	85	--	--	--
[8]	40×40	8 GHz	-20	--	--	5	--	85
[9]	38.5×38.5	8.72 GHz	-15	0.02	--	7.5	--	50
[16]	45×50	8.2 GHz	-25	0.02	76	4	1	85
[17]	30×60	7.5 GHz	-20	0.01	--	4.2	--	80
[22]	~90×90	9.4 GHz	-20	--	--	~5	--	--
PW	18×30	16.89 GHz	~-25	0.001	88.2	4.7	0.86	83

II. ANTENNA DESIGN AND CONFIGURATION

Figure 1 displays the geometry of the proposed antenna. It includes two similar monopoles that are perpendicular to each other and printed on FR4 substrate with thickness of 1.6 mm, relative permittivity of (εr =) 4.4 and loss tangent of (tanδ=) 0.02. Spacing between two monopole antennas (center to center) is 12 mm. Each antenna is fed by a width of 2 mm microstrip line in order to attain 50Ω input impedance.

The patch of the antenna consists of a Trapezius- and a rectangular-shape which is united together. The ground of antenna comprises a rectangular and two symmetrical L-shape slot inside it. Details of other dimension are given in Table 2. Figure 2 demonstrates the structure of the various antennas employed for simulation studies. S11 characteristics for ordinary square monopole antenna [Fig. 2 (step 1)], the antenna with an improved patch [Fig 2. (step 2)] and the proposed antenna by cutting ground [Fig. 2 (step 3)] structures are compared in Fig. 3. As shown in Fig. 3, by using the modified radiating patch and two L-shape slots in defected ground inserted on the other side of substrate, additional third and fourth resonances are excited respectively, and hence, the bandwidth is increased. As exposed in Fig. 3, in the offered antenna configuration, the ordinary square monopole can provide the fundamental and next higher resonant radiation band at 4 and 7.9 GHz, respectively, in the absence of two L-shaped slots and without modifying the edges of the patch. The upper frequency bandwidth is significantly affected by using the radiating patch because by improving the edge of the patch, surface current which is focused in the edge of the ordinary square patch (as seen in Fig. 4 (a)) is eliminated and, therefore, surface current spreads in the total surface of patch conductor (see Fig. 4 (b)). By inserting two L-shaped slots in ground plane, the antenna bandwidth increases. The two L-shaped slots prevent the spreading of power in microstrip feed line on the ground conductive surface and, also, causes an increase in the surface current rotation in ground conductive (see Fig. 4 (c)).

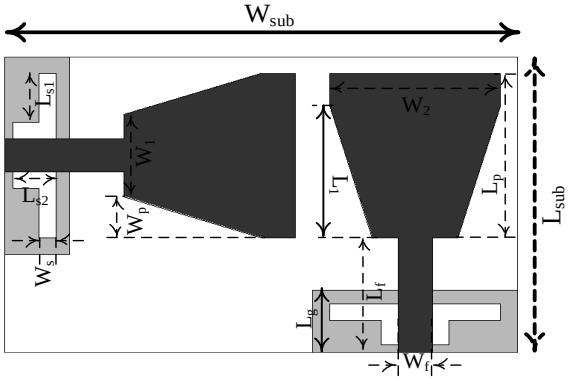

Fig. 1. Structure and dimension of proposed antenna.

Table 2: Parameters dimension

Parameter	Value	Parameter	Value
W_f	2 mm	W_1	5 mm
L_f	7 mm	W_2	10 mm
L_{s1}	3 mm	g	0.8 mm
L_{s2}	2.5 mm	h	1.6 mm
L_p	8 mm	W_{sub}	12 mm
W_p	2.5 mm	L_{sub}	17 mm
W_s	1 mm	L_g	3.8 mm

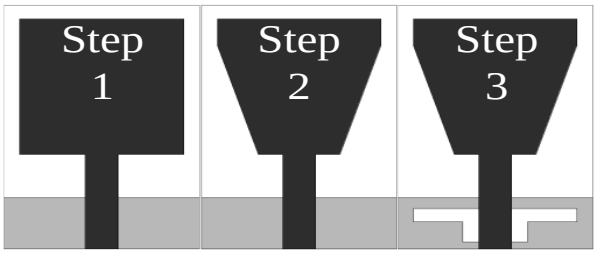

Fig. 2. Three steps of designing proposed monopole antenna.

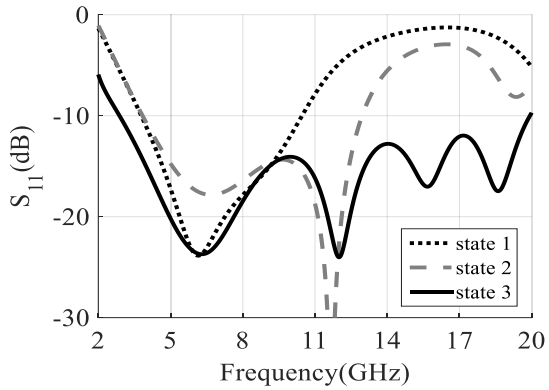

Fig. 3. Simulation S_{11} three steps of designing proposed monopole antenna.

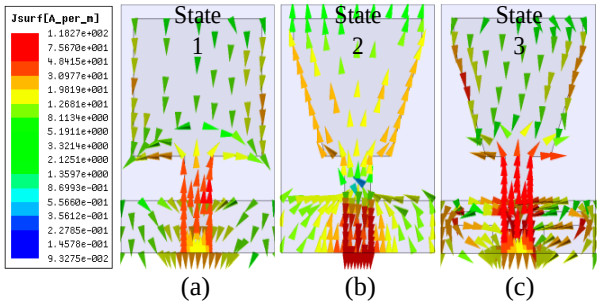

Fig. 4. Distribution of surface current: (a) simple square patch, (b) modified patch, and (c) modified ground and patch, at 8 GHz.

III. STUDY OF DGS EFFECT AT TDR

In order to comprehend defected ground structure effect in antenna performance Figs. 5 (a) and (b) are displayed. In order to calculate the TDR results for the proposed equivalent circuits, the impedance of these circuits in Laplace domain can be represented as in Equation (1):

$$Z_{DGS} = \frac{L_s+R}{LCs^2+RCs+1}. \quad (1)$$

Assuming that the characteristic impedance of the microstrip line is Z_0, we can write the reflection coefficient through a defected structure as in Equation (2), which is observed at the source end, i.e., port 1,

$$\Gamma_Z(s) = \frac{Z(s)}{Z(s)+2Z_0}. \quad (2)$$

Therefore, the reflected waveform for the proposed DGS can be written as:

$$\Gamma_{DGS}(s) = \frac{Ls+R}{2Z_0LCs^2+(2Z_0RC+L)s+R+2Z_0}. \quad (3)$$

A step voltage source with rise time τ_r and amplitude V0, can be expressed as in [18-21],

$$V_{in}(s) = \frac{V_0}{2\tau_r}\frac{1}{s^2}(1-e^{-(\tau_r s)}). \quad (4)$$

Therefore, the reflected waveform in Laplace domain can be written as:

$$V_{TDR}(s) = V_{in}(s)\Gamma_{DGS}(s). \quad (5)$$

In TDR measurements, the impedance follows as:

$$Z_{TDR} = \frac{Z_0(V_{in}(t)+V_{TDR}(t))}{V_{in}(t)-V_{TDR}(t)}. \quad (6)$$

In which Z_0 is the characteristic impedance of the transmission line at the terminal.

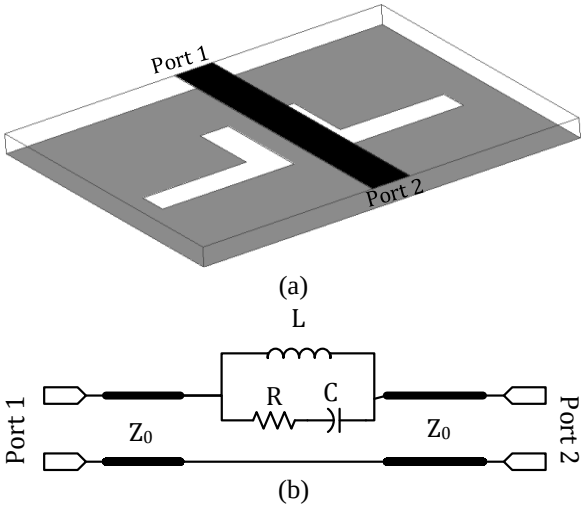

Fig. 5. (a) Geometry of the proposed DGS, and (b) equivalent circuit model.

The computed R, L and C of equivalent are 1.41Ω, 0.72nH and 16.01pF, respectively. In additionally, as mentioned with attention to LC circuit in equivalent circuit causes to creation of resonance in antenna performance.

IV. RESULT AND DISCUSSION

The proposed antenna was simulated by High Frequency Structure Simulator (HFSS) ver. 14, and then was optimized since the validation of results was fabricated and measured in frequency- and time-domain. In Fig. 6 (a) simulation results of insertion and isolation of two ports is indicated. As shown in this figure, simulated S11<-10 dB covered a frequency range from 2.98 to 20 GHz, and in this region of bandwidth, simulated S21 is less than about -25 dB. Scattering parameters of antenna was measured using Agilent EM 8722ES vector network analyzer. Measured results of S11 and S12 are

displayed in Fig. 6 (b). By comparing simulation and measured scattering results, it can be concluded that there is good matching between them in the expanding region. Measured results indicate that the antenna supplies an impedance bandwidth (S11&S22≤-10 dB) from 2.97 to 19.86 GHz, and it can also be realized that the measured port isolations (S21 & S12) are less than about -25 dB throughout the band. Thus, the bandwidth prerequisite for UWB applications is realized. Due to the effects of manufacturing tolerance, imperfect solder joints of the SMA connector to the feed-line and measurement environment, measured port is slightly worse than the simulation at frequencies from 3 to 11 GHz. Figure 7 depicts measured radiation patterns at 3, 6, 10, 14, and 19 GHz when port 2 is excited, while port 1 is terminated with a 50Ω load, and vice versa.

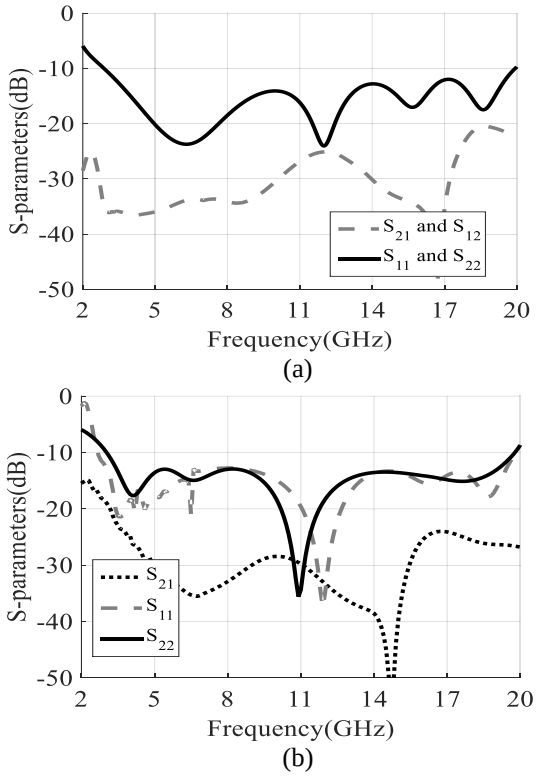

Fig. 6. Comparison between simulated and measured S11, S22 and S21: (a) Simulated and (b) measured.

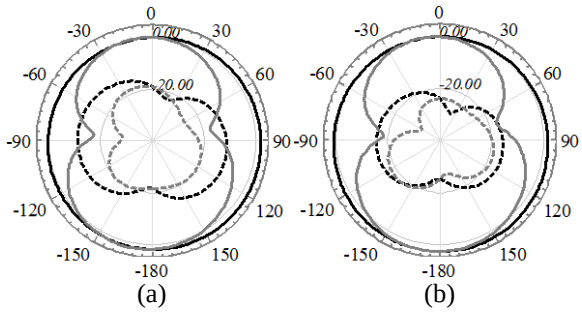

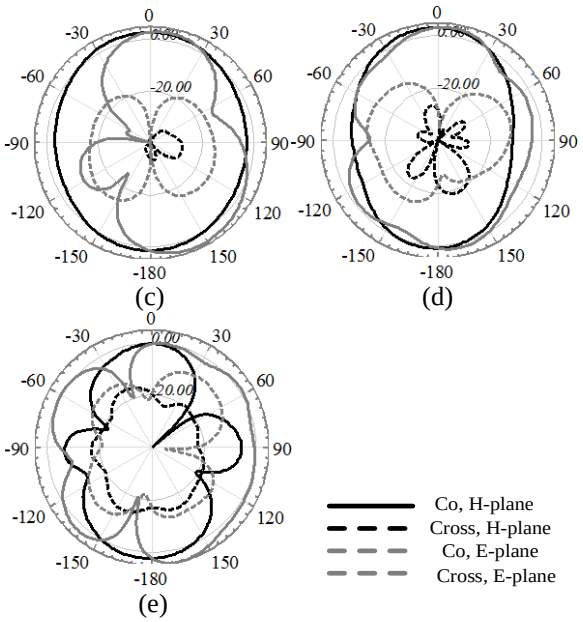

Fig. 7. Depicts measured radiation patterns at 3, 6, 10, 14 and 19 GHz when port 2 is excited: (a) 3 GHz, (b) 6 GHz, (c) 10 GHz, (d) 14 GHz, and (e) 19 GHz.

Figure 8 illustrates the simulated electric field distribution at 4, 8, and 12 GHz of the diversity antenna when two ports are excited respectively at different frequencies. It can be observed that the electric field is X-direction when port 1 is excited while the electric field shifts to Y-direction when port 2 is excited, which is consistent with the aforementioned current analysis. However, the polarization worsens at high frequency, which is attributed to the complicated current distribution on the radiator [8]. Gains and radiation efficiencies of the antennas for port 1 and 2 are measured. Figure 9 shows the measured gains of two antenna elements within the UWB band that are larger than 3.8 dB and have a peak gain of 4.7 dBi.

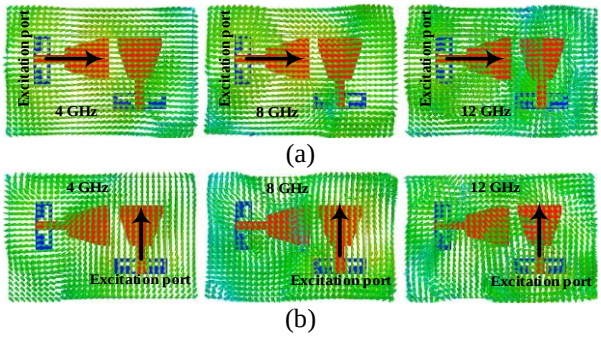

Fig. 8. The simulated far field electric field distribution at 4, 8, and 12 GHz of the diversity antenna when two ports are excited: (a) port 1 directed in X-direction, and (b) port 2 directed in Y-direction.

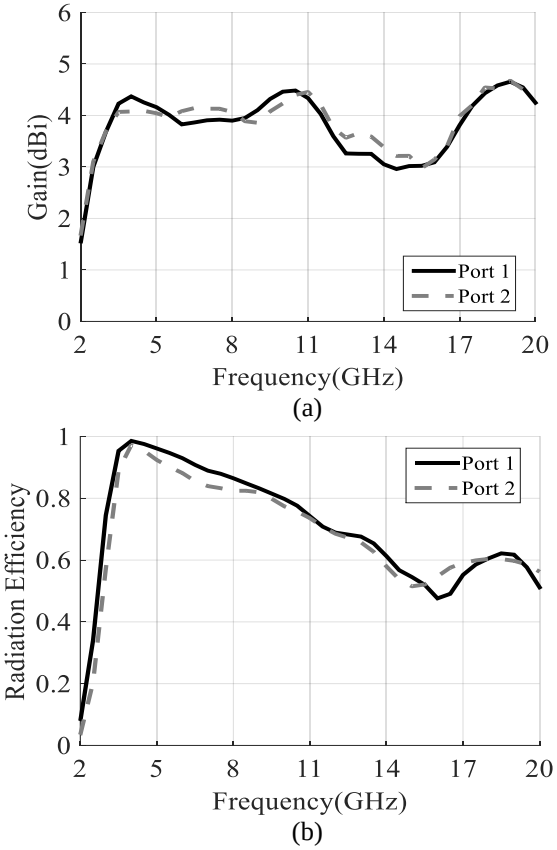

Fig. 9. Measured gains and radiation efficiencies of antennas for port 1 and 2: (a) gain and (b) radiation efficiencies.

It is essential to evaluate the Envelope Correlation Coefficient (ECC) since an ECC greater than 0.05 (less than -13 dB) can typically degrade the diversity performance. The ECC of the proposed antenna is also calculated [10, 23] using:

$$\rho_e = \frac{|S_{11}^* S_{12} + S_{21}^* S_{22}|^2}{(1-(|S_{11}|^2+|S_{21}|^2))(1-(|S_{22}|^2+|S_{12}|^2)}, \quad (7)$$

and is plotted in Fig. 10. The measurement and simulated values of ECC remain low throughout the UWB spectrum, which indicates that the proposed antenna is a good candidate for wireless communication systems with polarization diversity.

In a UWB system, the antenna needs to possess a high level of pulse-handling capability to handle high-frequency impulses. Hence, the time-domain properties are equally as important as frequency domain [1]. The group delay of the antenna is measured by exciting two identical antennas kept in the far field with face-to-face orientation (when one of the ports is excited, another port is terminated with 50 load, and vice versa). It is clear from Fig. 11 that the antenna displays a group delay that remains almost constant with variations less than 1 ns.

The HFSS default Gaussian pulse with spectrum covering from 2 GHz to 20 GHz band was employed as the input signal, as it completely complies with the FCC indoor and outdoor power masks [15]. Figure 12 displays the antenna impulse reply for the two measured directions.

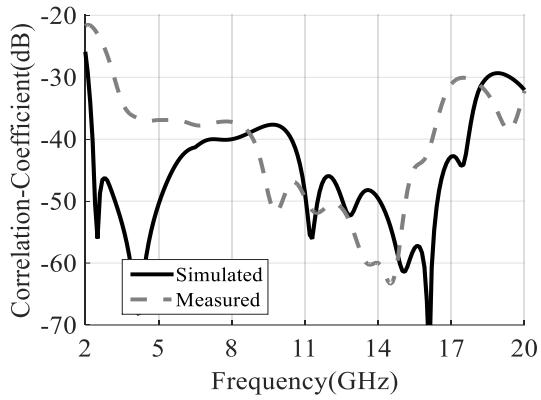

Fig. 10. Comparison between simulation and measurement values of ECC.

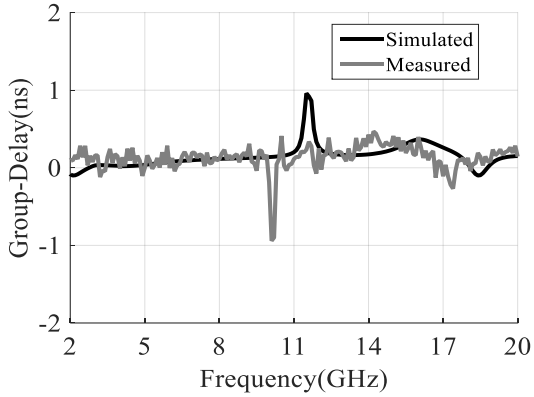

Fig. 11. Comparison between simulation and measurement values of proposed antenna group delay.

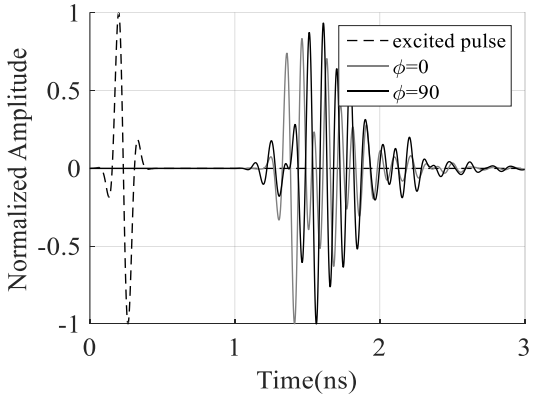

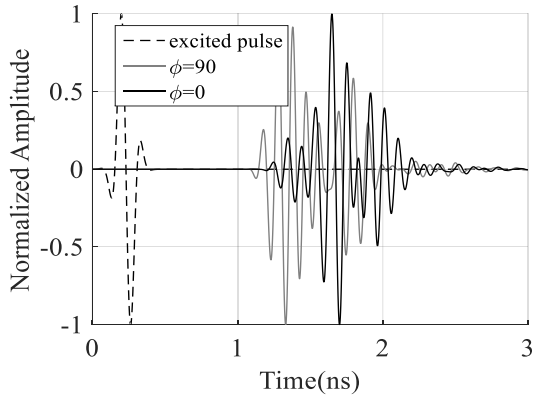

Fig. 12. Normalized amplitude measurement of Gaussian pulse response of antenna.

To compute the level of distortion, the system fidelity factor has been considered as in [14], and results are specified in Table 3. The measured average system fidelity factors, for the considered directions, of ports 1 and 2 are 88.2% and 84.3%, respectively, which shows that the level of signal distortion is quite suitable for UWB signals transmission [7]. The footprint of fabricated proposed compact polarization diversity MIMO antenna is illustrated in Fig. 13.

Table 3: Measured of system fidelity factor

Port 1	φ=0	89.6%
	φ=90	86.8%
Port 2	φ=0	85.3%
	φ=90	83.2%

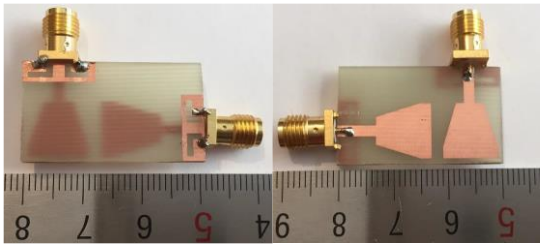

Fig. 13. Photograph of fabricated antenna.

V. CONCLUSION

An UWB MIMO antenna for polarization diversity applications has been proposed. The antenna prototype (with a size of 18×30 mm^2) in compared with same articles [1-9] have very compacted size and better results. Results show that the proposed antenna achieves an impedance bandwidth of larger than 147.96% (2.97 to 19.86 GHz). A high isolation between two ports has been achieved. Besides, low envelope correlation coefficient less than 0.001 was obtained. In the future, the proposed diversity UWB antenna mentioned above can be a promising candidate for wireless communication systems where a challenge such as multipath fading is a major concerns.

REFERENCES

[1] B. P. Chacko, G. Augustin, and T. A. Denidni, "Uniplanar slot antenna for ultrawideband polarization-diversity applications," in *IEEE Antennas and Wireless Propagation Letters*, vol. 12, pp. 88-91, 2013.

[2] S. Zhang, B. K. Lau, A. Sunesson, and S. He, "Closely-packed UWB MIMO/diversity antenna with different patterns and polarizations for USB dongle applications," in *IEEE Transactions on Antennas and Propagation*, vol. 60, no. 9, pp. 4372-4380, Sept. 2012.

[3] H. Huang, Y. Liu, S. Zhang, and S. Gong, "Uniplanar ultrawideband polarization diversity antenna with dual band-notched characteristics," in *IEEE Antennas and Wireless Propagation Letters*, vol. 13, pp. 1745-1748, 2014.

[4] H. Huang, Y. Liu, and S. Gong, "Uniplanar differentially driven UWB polarisation diversity antenna with band-notched characteristics," in *Electronics Letters*, vol. 51, no. 3, pp. 206-207, Feb. 5, 2015.

[5] B. P. Chacko, G. Augustin, and T. A. Denidni, "Uniplanar polarisation diversity antenna for ultrawideband systems," in *IET Microwaves, Antennas & Propagation*, vol. 7, no. 10, pp. 851-857, July 16, 2013.

[6] H. Huang, Y. Liu, S. Zhang, and S. Gong, "Uniplanar differentially driven ultrawideband polarization diversity antenna with band-notched characteristics," in *IEEE Antennas and Wireless Propagation Letters*, vol. 14, pp. 563-566, 2015.

[7] M. Koohestani, A. A. Moreira, and A. K. Skrivervik, "A novel compact CPW-fed polarization diversity ultrawideband antenna," in *IEEE Antennas and Wireless Propagation Letters*, vol. 13, pp. 563-566, 2014.

[8] C. X. Mao and Q. X. Chu, "Compact co radiator UWB-MIMO antenna with dual polarization," in *IEEE Transactions on Antennas and Propagation*, vol. 62, no. 9, pp. 4474-4480, Sept. 2014.

[9] L. Kang, H. Li, X. Wang, and X. Shi, "Compact offset microstrip-fed MIMO antenna for band-notched UWB applications," in *IEEE Antennas and Wireless Propagation Letters*, vol. 14, pp. 1754-1757, 2015.

[10] W. K. Toh, Z. N. Chen, Q. Xianming, and T. S. P. See, "A planar UWB diversity antenna," *IEEE Trans. Antennas Propag.*, vol. 57, no. 11, pp. 3467-3473, Nov. 2009.

[11] Q. H. Abbasi, M. M. Khan, S. Liaqat, M. Kamran, A. Alomainy, and Y. Hao, "Experimental investigation of ultra wideband diversity techniques for

on-body radio communications," *Prog. Electromagn. Res. C*, vol. 34, pp. 165-181, 2013.

[12] Q. H. Abbasi, A. Alomainy, and Y. Hao, "Ultra wideband antenna diversity techniques for on/off-body radio channel characterization," in *Proc. IEEE iWAT*, pp. 209-212, 2012.

[13] Y. Li, W. X. Li, Ch. Liu, and T. Jiang, "A printed diversity cantor set fractal antenna for ultra wideband communication applications," in *Proc. Antennas, Propag., EM Theory*, pp. 34-38, 2012.

[14] G. Quintero, J.-F. Zürcher, and A. K. Skrivervik, "System fidelity factor: A new method for comparing UWB antennas," *IEEE Trans. Antennas Propag.*, vol. 59, no. 7, pp. 2502-2512, July 2011.

[15] M. Koohestani, N. Pires, A. K. Skrivervik, and A. A. Moreira, "Time domain performance of patch-loaded band-reject UWB antenna," *Electron. Lett.*, vol. 49, no. 6, pp. 385-386, 2013.

[16] B. S. Femina and S. K. Mishra, "Compact WLAN band-notched printed ultrawideband MIMO antenna with polarization diversity," in *Progress In Electromagnetics Research C*, vol. 61, pp. 149-159, 2016.

[17] H. Huang, Y. Liu, S.-S. Zhang, and S.-X. Gong, "Compact polarization diversity ultrawideband mimo antenna with triple band-notched characteristics," *Microw. Opt. Technol. Lett.*, vol. 57, iss. 4, pp. 946-953, Apr. 2015.

[18] M. Ojaroudi and E. Mehrshahi, "Bandwidth enhancement of small square monopole antennas by using defected structures based on time domain reflectometry analysis for UWB applications," *Applied Computational Electromagnetics Society Journal*, vol. 28, iss. 7, pp. 620-627, July 2013.

[19] R. Azim, M. T. Islam, and N. Misran, "Design of a planar UWB antenna with new band enhancement technique," *Appl. Comp. Electro. Society (ACES) Journal*, vol. 26, no. 10, pp. 856-862, Oct. 2011.

[20] G. Zhang, J. S. Hong, B. Z. Wang, and G. Song, "Switched band-notched UWB/ WLAN monopole antenna," *Appl. Comp. Electro. Society (ACES) Journal*, vol. 27, no. 3, pp. 256-260, Mar. 2012.

[21] W. C. Weng, "Optimal design of an ultra-wideband antenna with the irregular shape on radiator using particle swarm optimization," *Appl. Comp. Electro. Society (ACES) Journal*, vol. 27, no. 5, pp. 427-434, May 2012.

[22] X.-S. Yang, S.-G. Qiu, and J.-L. Li, "Triangular-arranged planar multiple-antenna for UWB-MIMO applications," *Applied Computational Electromagnetics Society Journal*, vol. 29, iss. 1, pp. 62-66, Jan. 2014.

[23] P. Zibadoost, J. Nourinia, C. Ghobadi, S. Mohammadi, A. Mousazadeh, and B. Mohammadi, "Full band MIMO monopole antenna for LTE systems," *Applied Computational Electromagnetics Society Journal*, vol. 29, iss. 1, pp. 54-61, Jan. 2014.

Saeid Karamzadeh received his M.S. and Ph.D. degrees in Department of Communication Systems, Satellite Communication & Remote Sensing program at Istanbul Technical University in 2013 and 2015 respectively. He won the most successful Ph.D. thesis award of Istanbul Technical University. Currently, he is an Assistant Professor in the Istanbul Aydin University, Department of Electrical and Electronics Engineering. He is also with Application & Research Center for Advanced Studies in the Istanbul Aydin University, Turkey. His research interests include remote sensing, radar, microwave, and Antenna design.